Prediction of mechanical properties of nylon and polyester fibres as composites

J. W. S. Hearle, R. Prakash and M. A. Wilding
Department of Textiles, University of Manchester Institute of Science and Technology, Manchester, UK

(*Received 21 April 1986*)

The structure of melt-spun fibres is treated as identical cuboidal crystals in an isotropic rubbery matrix. Approximate initial moduli and tensile relations are derived using three approaches: first, using an arbitrary weighting factor describing the relative proportions of series- and parallel-coupled material. Both modulus and compliance averaging procedures are performed. Secondly, Takayanagi's unit cell method is applied to a series followed by a parallel system, then *vice versa*. Thirdly, the structure is regarded as a filled rubber with the crystals as filler particles. Guth's analysis, where the matrix strain is enhanced by the filler particles, is applied. Results from these methods are compared, and the roles of crystallinity and crystal aspect ratio examined.

(Keywords: composites; structure modelling; mechanical properties; tensile modulus; stress–strain curve; melt-spun fibres)

INTRODUCTION

The structure of melt-spun synthetic fibres, such as nylon-6,6, nylon-6, and polyester [poly(ethylene terephthalate)] is generally assumed to consist of crystalline micelles, with some fringing into tie-molecules and some folding, stacked in a pseudo-fibrillar array in a matrix of amorphous material. A typical qualitative representation of the structure is shown in *Figure 1*, from Hearle and Greer[1], but similar models have been given by Peterlin[2], Prevorsek[3] and Statton[4]. However no treatments of the mechanics of such a structure have been published. Although there is a need for a more quantitative characterization of the structure before good theoretical predictions can be made, and we are presently examining this aspect of the subject, an initial examination of the mechanics of the simple model regarded as a composite of micelle and matrix following the suggestions of Takayanagi[5] has shown up a number of interesting features: in particular, different treatments which might seem to be similar turn out to depend on different parameters. The paper is particularly appropriate for this commemoration issue, because of Treloar's pioneering calculations of the elastic moduli of polymer crystals[6] and the stress–strain relations of crosslinked rubbers[7], which are the two components of the system.

There are three types of problems associated with the analysis. Firstly, there are the formidable problems of the mechanics of any composite system, except for some simple special cases. Secondly, there is the problem of knowing the mechanical properties of the component crystalline and amorphous structures. These two areas are, approximately, dealt with in this paper. But, thirdly, there are important features of real fibres which would need to be considered in a more exhaustive theoretical treatment. These include:

(a) crystalline orientation and form—the crystals are regarded as lined up uniaxially, so that no elongation is possible through rotation of the crystal axis, and there is a tacit assumption that all the crystals are of the same size and equally spaced in a regular pattern;

(b) amorphous orientation and form—the amorphous matrix is tacitly assumed to be isotropic, and to be an idealized network with no bias imposed when it was formed;

(c) tie molecules—the two components are assumed to be independent materials, whereas in reality the chain molecules pass continuously through both, with some free chain ends;

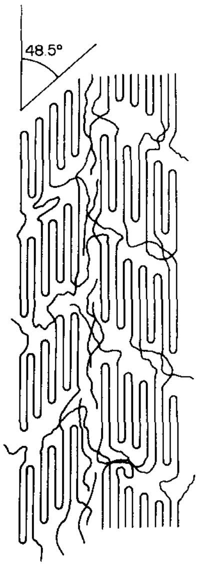

Figure 1 Commonly accepted model of fine structure of melt-spun fibres, after Hearle and Greer[1]

0032–3861/87/030441–08$03.00

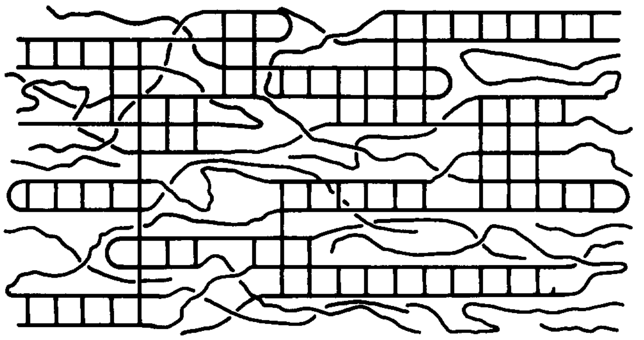

Figure 2 Alternative views of structure, after Hearle and Greer[1]

(d) molecular dimensions—each component is taken to be a mechanical continuum, whereas in reality the dimensions of the polymer units are less than an order of magnitude smaller than the scale of the structure;

(e) differences in essential structure—there are alternative views of structure, illustrated in *Figure 2.* These are more continuous forms, without clear boundaries between crystalline and amorphous material. They do not approximate to the forms of *Figure 1,* and would not lead to a simple two-component composite analysis; but they may be valid at least in some circumstances;

(f) transverse and shear strains—only tensile strains are taken into account, and the inclusion of amorphous material within a 'box' defined by the crystallites is neglected.

THEORETICAL CONSIDERATIONS

Crystalline phase

The crystal lattice is a well-defined form, and, at least in principle, the elastic constants can be calculated theoretically from inter-atomic forces or potentials, and in some instances experimental estimates of the moduli of polymer crystals have been derived from lattice strains estimated from changes in the diffraction pattern. *Table 1* lists some relevant estimates of the axial crystal modulus E_c.

Amorphous phase

A simplistic two-dimensional view of the disordered material, as it might exist in nylon-6 is shown in *Figure 3.*

In nylon-6 there is an alternation along the chains of a methylene sequence, $(-CH_2-)_5$, and an amide group, $-CO.NH-$. Bond rotation is relatively easy within the methylene sequence and there are only weak van der Waals interactions laterally. Some bond rotation is possible in the amide group, but hydrogen bonding may occur laterally with neighbouring chain segments. Nylon-6,6 would have the trivial differences that the $-CH_2-$ groups alternated in blocks of 4 and 6, and that the $-CO.NH-$ groups alternately reversed direction.

In polyester there is instead an alternating sequence of an ester grouping, $-OOC.(CH_2)_2.COO-$, and a benzene ring. Bond rotations will again be relatively easy within the ester group, and lateral interactions will be primarily weak van der Waals forces (although it is possible that some dipolar effects may be associated with the carbonyl groups). On the other hand, the benzene ring is an extremely rigid entity, and interactions can occur between adjacent rings.

The important common feature of all these types of polymeric fibres is that there is an alternation of flexible and more interactive linkages along the chains.

For convenience, the behaviour of amorphous materials might be summarized in terms of several regions, with transitions occurring at some temperature between those mentioned:

At very low temperatures (less than −100°C) there would be no freedom of rotation around the main chain bonds, and the amorphous material would be glassy. According to a crude theoretical treatment by Hearle[8], the modulus E_g would be given by:

$$E_g = (p/n^2)\bar{E}_c \tag{1}$$

Table 1 Crystalline moduli (in GPa) of some polymers

Polymer	Modulus	Method used	Reference
Nylon-6,6	157	Force constants	14
	196	Force constants	6
Polyethylene	102	Force constants	6
	324	Lattice dynamics	15
Polyester	146	Force constants	14
	137	X-rays	16
	122	Force constants	6
	122	Force constants	6
Cellulose	57	Force constants	6

Note: (1) Full treatments include a full set of anisotropic elastic constants

(2) For specific values in N/tex divide by density in g cm^{-3}: nylon-6 and nylon-6,6, 1.22; poly(ethylene terephthalate), 1.45; polyethylene, 1.0

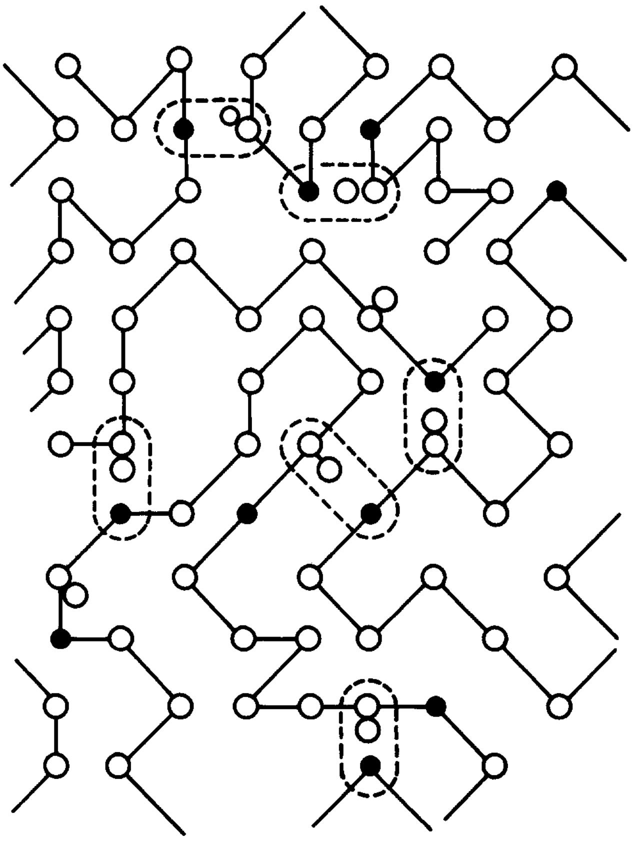

Figure 3 Schematic (two-dimensional), representation of amorphous structure; Hearle[13]

where p is a geometrical parameter related to the distribution of stress and strain in the structure, n is the number of links which can deform as an independent unit, and $\bar{E}_c$ is the average crystal modulus.

For our purposes, we could put:

$$E_g = QE_c \tag{2}$$

where Q (with a value of about 0.1) is a measure of the reduction in stiffness due to the irregular conformation, and E_c is the *axial* crystal modulus.

At intermediate temperatures (around 20°C) in nylon and polyester, there will be freedom of rotation around the aliphatic main chain bonds. However in nylon, the hydrogen bonding between –CO.NH– groups would be held, so that the material would behave like a rather highly crosslinked rubber with about 6 C–C bonds between network junctions: this is equivalent to about 2 freely-jointed random links. The rubber elasticity theory predictions are dealt with in the next section.

Polyester could be regarded in a similar same way, as mentioned already, with 7 bonds in the aliphatic sequence and the junctions attributed to strong electronic interaction between the benzene rings. Alternatively, the large stiff benzene rings may be regarded as inhibiting chain movement through geometrical blocking or entanglement. The presence of the benzene rings (providing half the main chain atoms) must, in any case, have a stiffening effect on the rubbery network.

At higher temperatures still (about 120°C) the hydrogen bonds in nylon will be subject to rupture by thermal vibration and the amorphous material would be in a liquid-like state of dynamic equilibrium. However the ends of chain segments would still be held in the crystals, so that (straining the continuum approximation harder) the amorphous material could be regarded as a rubber with chain lengths between junction points of the order of the spacing between crystals. This would be about 10 nm, giving about 80 main chain bonds, or 25 random links. Subject to the same reservations as before concerning the influence of the benzene rings, polyester could be regarded as similar, when the chains become free to move relative to one another (at a higher temperature than in nylon).

At still higher temperatures (around 200°C in nylon-6,6 and polyester, and 150°C in nylon-6) mobility will begin to develop in the crystals as a prelude to crystal melting at a higher temperature.

According to the nonlinear theory of rubber elasticity derived independently by Kuhn and Grun[9] and by James and Guth[10] the specific stress* on a single rubbery chain is given by:

$$f = (kT/m_0)[\mathrm{arc}\,\mathscr{L}(l/L)] \tag{3}$$

where m_0 = mass of one equivalent random link in the chain, k = Boltzmann's constant, T = temperature (K), l = distance between chain ends, L = fully extended length of chain and $\mathrm{arc}\,\mathscr{L}(x)$ is the inverse of the Langevin function $\mathscr{L}(x) = \coth(x) - (x)^{-1}$.

Equation (3) can be expanded as:

$$f = (3kT/m_0)[(l/L) + (3/5)(l/L)^3 + (99/175)(l/L)^5 + \ldots] \tag{4}$$

For a solid network of rubbery chains, the simplest theory for prediction of moduli is based on the first (linear) term in the above series (which can also be derived from Gaussian statistics) and on affine deformation of a uniform network. The shear modulus G, and the tensile modulus, E_r of the rubber are then given by:

$$G = 1000\,\rho RT/M_c \tag{5a}$$

$$E_r = 3000\,\rho RT/M_c \tag{5b}$$

where ρ = density (kg m^{-3}), $R = 8.3\,\mathrm{J\,K^{-1}\,mol^{-1}}$ and M_c = number-average molecular weight of the chain segments between crosslinks.

With ρ at the approximate value of 1000 kg m^{-3} and T at the approximate value of 300 K, this gives:

$$E_r = (7.5/M_c)\ \mathrm{GPa\ or\ N/tex}$$

For larger strains, it is necessary to take account of non-linearity. Computation would allow equation (3) to be used in affine deformation of the network, but for the approximate treatment here, it is convenient to use one of the earlier algebraic forms.

Treloar[7] gives the following expression for the affine deformation of the network, using the series expansion in equation (4):

$$f = G\left(\lambda - \frac{1}{\lambda^2}\right)\left[1 + \frac{3}{25n}\left(3\lambda^2 + \frac{4}{\lambda}\right) + \ldots\right] \tag{6}$$

where λ = extension ratio = 1 + strain, n = number of random links between junction points.

Note that (in contrast to the independence of the modulus) the onset of nonlinearity does depend on the effective size of a random link.

To the nearest order of magnitude (which is all that is justified in the present general treatment) the modulus values of the two components may be summarized as in *Table 2*.

THE COMPOSITE SYSTEM

Approach I: parallel and series influence

There are two composite systems which are easy to analyse, namely the series and parallel models shown in *Figure 4*(*a*) and (*c*). For the parallel model, the weighted mean stress is calculated for the two components under the same strain; and for the series model the weighted mean strain is calculated for the two components under

Table 2 Modulus values of the two components

Crystal E_c	Crystal modulus	10^{11} Pa	(100 GPa or N/tex)
Amorphous E_a	Low temperature (−100°C) QE_c	10^{10} Pa	(10 GPa or N/tex)
	Room temperature $7.5/M_c$ GPa, $M_c \simeq 100$	10^8 Pa	(0.1 GPa or N/tex)
	Higher temperature (150°C) $7.5/M_c$ GPa, $M_c \simeq 1000$	10^7 Pa	(0.01 GPa or N/tex)

---

* Specific stress = force/linear density = stress/density, and the SI units are N/(kg m^{-1}), J/kg or Pa/(kg m^{-3}). In fibre usage, the preferred units are N/tex = N/(g/km).

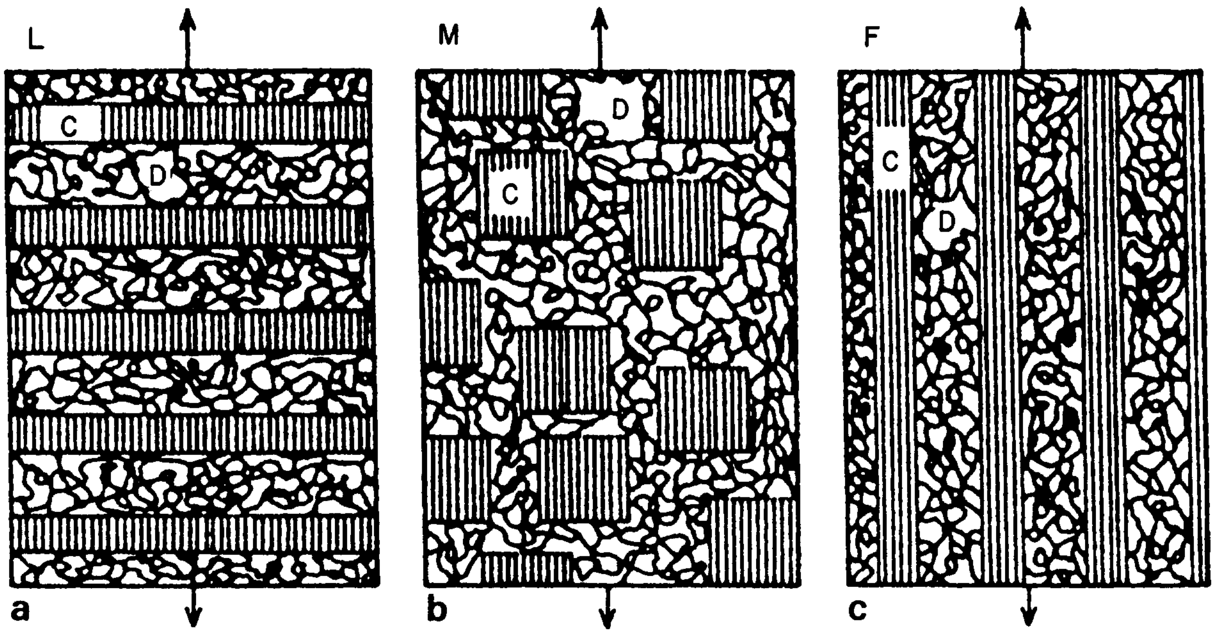

Figure 4 Models used by Hearle[13] in a treatment of mechanics of rayon fibres: (a) lamellar, series; (b) micellar; (c) fibrillar, parallel

the same stress. The moduli are thus given by:

$$\text{parallel} \quad E_p = X_c E_c + (1 - X_c) E_a \qquad (7)$$

$$\text{series} \quad E_s = [X_c E_c^{-1} + (1 - X_c) E_a^{-1}]^{-1} \qquad (8)$$

where $E_a = E_g$ or E_r, the amorphous modulus; X_c = crystalline fraction (volume fraction for moduli, mass fraction for specific moduli).

The stress–strain equations that would be used for the non-linear relations are

$$\text{parallel} \quad f_p = X_c f_c(\varepsilon) + (1 - X_c) f_a(\varepsilon) \qquad (9)$$

$$\text{series} \quad \varepsilon_s = X_c \varepsilon_c(f) + (1 - X_c) \varepsilon_a(f) \qquad (10)$$

where $f_c(\varepsilon)$ and $f_a(\varepsilon)$ are the stress–strain curves and $\varepsilon_c(f)$ and $\varepsilon_a(f)$ are the inverse relations.

The intermediate micellar form, *Figure 4(b)*, which is represented in its simplest form by a repetition of the unit shown in *Figure 5a*, is more difficult to analyse since it must involve variations in tensile strain and shear strain through each component.

We can consider various ways of dealing with the problem. One is the somewhat arbitrary procedure of using a weighting factor P to define the relative influence of the parallel and series components. P will approach 1 as $L_c/B_c \to \infty$ and approach 0 as $L_c/B_c \to 0$; and for a micellar system would be around 0.5.

However the average can be taken in different ways, with the two simplest being an appropriate weighting of either modulus or compliance:

$$E_m = P E_p + (1 - P) E_s \qquad (11)$$

or

$$E_m^{-1} = P E_p^{-1} + (1 - P) E_s^{-1} \qquad (12)$$

The non-linear stress–strain relations might be determined roughly by using the value of E_m as a modified front factor in equation (6); but it could also be given more correctly by combining the parallel and series equations (9) and (10) in either of the two ways used for the modulus in equations (11) or (12).

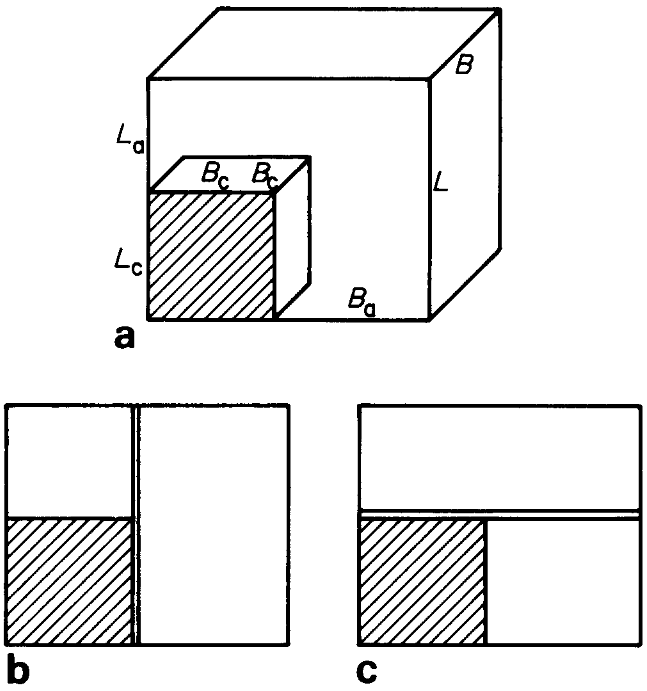

Figure 5 (a) Representative cell of micellar model. (b) Series followed by parallel. (c) Parallel followed by series

Approach II: sequential operation on model

The second approach following Takayanagi[5] takes the representative unit shown in *Figure 5a* and then analyses its response in sequence *either*, as in *Figure 5b*, as two units in series followed by two units in parallel, *or*, as in *Figure 5c*, as two units in parallel followed by two units in series.

The first stage is to calculate the moduli of the parallel and series arrangements separately. These may be

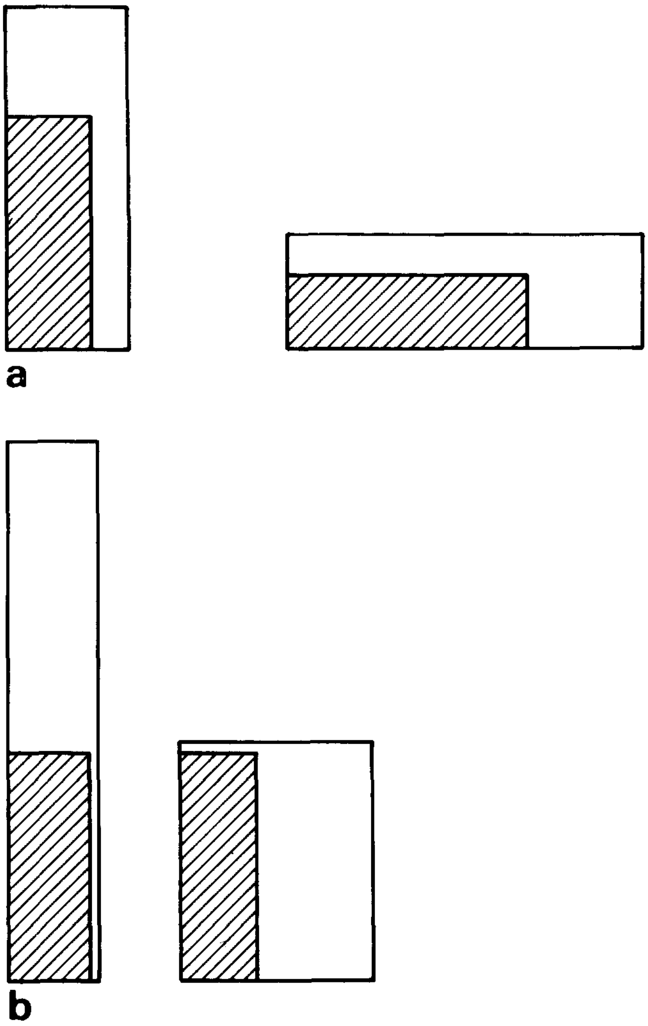

Figure 6 (a) Two different geometries, giving the same prediction on Approach II, both having $L_c/B_c = 2/3$ and $X_c = 4/9$ (in 2-D form). (b) Two different geometries giving the same prediction on Approach III, both having $L_c/B_c = 3$ and $X_c = 4/9$ (in 2-D form)

expressed in terms of the crystallite's fractional length, ϕ, and fractional breadth (for a 2-dimensional, 2-D, unit cell) or area of cross-section (for a 3-dimensional, 3-D, unit cell), β, as:

$$E_{mp} = \beta E_c + (1-\beta)E_a \tag{13}$$

$$E_{ms} = \{\phi E_c^{-1} + (1-\phi)E_a^{-1}\}^{-1} \tag{14}$$

where $\phi = L_c/L$; $\beta = B_c/B$ (2-D case)

$$\beta = B_c^2/B^2 \text{ or } A_c/A \text{ (3-D case)}$$

(A represents area)

It follows that: $X_c = \phi\beta$

The second stage leads to moduli expressions of a parallel–series and series–parallel aggregate as follows:

$$E_{mps}\{\phi E_{mp}^{-1} + (1-\phi)E_a^{-1}\}^{-1}$$

$$= \frac{X_c E_c E_a + (\phi - X_c)E_a^2}{(1-\phi)X_c E_c + (\phi - X_c + X_c\phi)E_a} \tag{15}$$

$$E_{msp} = \{\beta E_{ms} + (1-\beta)E_a\}$$

$$= \frac{(1-\phi+X_c)E_c E_a + (\phi - X_c)E_a^2}{\phi E_a + (1-\phi)E_c} \tag{16}$$

It is interesting to note that the values of E_{mps} and E_{msp} depend on only two geometrical parameters, e.g. ϕ and X_c, whereas the geometrical characterization requires three parameters. There may be some value in using a parameter such as $\gamma = \phi/\beta$, which indicates the relative amounts of amorphous material distributed axially and transversely between crystallites. This means that the different forms shown in *Figure 6*(*a*) would give the same predicted moduli on this approach. The predicted moduli are independent of the ratio L_c/B_c in the crystallites, and depend only on the relative lengths of crystalline section to amorphous section in each direction. The moduli would be different if account was taken of the interaction between the two components, particularly if there was staggering of the packing of the micelles.

The predicted non-linear stress–strain curves could again be given by using the calculated moduli to modify the front factor in equation (6); but would be more correctly calculated from a sequential combination (analogous to that for modulus) of equations of the form of equations (13) and (14).

An interesting variation of this approach is to treat the assembly as a continuous crystalline phase with amorphous inclusions. This then leads to a similar set of equations, but with the E_a and E_c terms interchanged.

Approach III: following Guth

Another approach is to use a relation proposed by Guth[11] quoted by Mullins and Tobin[12] and successfully applied to vulcanized rubbers containing fillers. In contrast to the previous approach, this depends on the ratio L_c/B_c and the crystallinity X_c and would be independent of how the amorphous material was distributed, so that the two geometries in *Figure 6*(*b*) would give the same prediction. The filled rubbers would naturally be midway between the extremes. The approach is based on the extension ratio, λ, and assumes that in order to calculate the stress, the stain must be enhanced, in comparison with the pure rubber where $\lambda = 1 + \varepsilon$, by a factor ($FR$) included through the expression:

$$\lambda = 1 + (FR)\varepsilon \tag{17}$$

Guth gives the following expression:

$$FR = 1 + 0.67\, X_c(L_c/B_c) + (1.62)\, X_c^2\, (L_c/B_c)^2 \tag{18}$$

The stress–strain curve is simply given by changing the strain scale of the rubber elasticity equation (6) by the factor (FR). The modulus will be $(FR)E_a$.

Table 3 gives values of (FR) for different values of X_c and L_c/B_c. The constant prediction of $(FR) = 1$ for $X_c = 0$ is, by definition, correct. The values of (FR)for $X_c = 1$ are clearly wrong since this should lead constantly to the crystal modulus. Generally the predictions for high values of X_c and L_c/B_c are likely to be suspect because they should be strongly influenced by the crystal modulus which is not included in the equations.

Table 3 Values of (a) FR, and (b) L_c/B_c, derived according to equation (18)

(a) L_c/B_c	X_c (1)	0.8	0.5	0.2	(0)
100	(16300)	10400	4080	662	(1)
10	(170)	110	44.8	8.82	(1)
5	(44.8)	29.6	12.8	3.29	(1)
2	(8.82)	6.22	3.29	1.53	(1)
1	(3.29)	2.57	1.74	1.20	(1)
0.5	(1.74)	1.53	1.27	1.08	(1)
0.2	(1.20)	1.15	1.08	1.03	(1)
10^{-1}	(1.08)	1.06	1.04	1.01	(1)
10^{-2}	(1.01)	1.0	1.0	1.0	(1)

(b) FR	X_c 0.2	0.5	0.8
1	0	0	0
10	10.8	4.3	2.7
100	38.1	15.2	9.5
1000	123.1	49.2	30.8

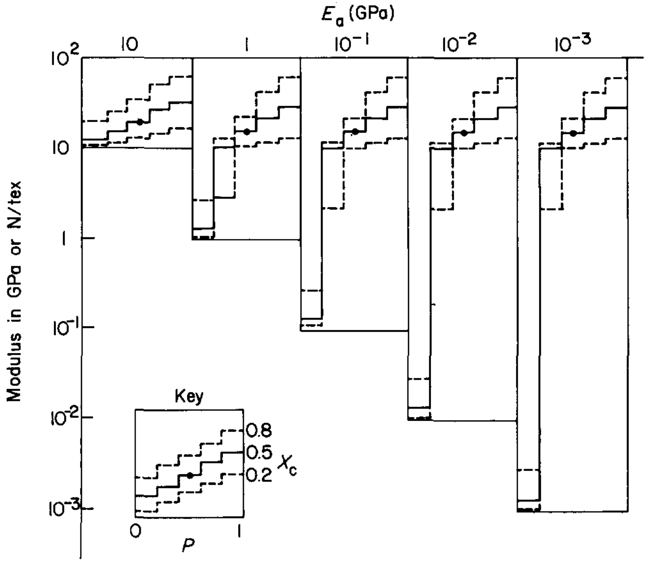

Figure 7 Computed initial modulus values under Approach I (based on weighted average of modulus), presented as function of amorphous modulus, E_a, and for a fixed crystal modulus, E_c '100 GPa or N/Tex). Each set of values shows effect of crystallinity, X_c, and degree of parallel and series influence, P, on composite modulus, e.g. solid line with a dot (–●–) represents modulus value for $P=0.5$ and $X_c=0.5$

RESULTS AND DISCUSSION

Figures 7 and *8* summarize the results using approach I, namely an arbitrary combination of parallel and series influence, with the two alternative modes of combination (average modulus and average compliance).

Figures 9 and *10* summarize the results using approach II. Note that a value of $\phi=X_c$ implies that all the amorphous material is in series, and a value of $\phi=1$ implies that all the amorphous material is in parallel. The intermediate values cover the range from series to parallel with $\phi=X_c^{1/2}$ meaning that the amorphous material is equally distributed around the crystallites.

Figure 11 summarizes the results using approach III for a set of values of L_c/B_c and X_c. *Figure 12* gives the same information plotted against FR on a log scale.

Experimental modulus values for nylon and polyester cover a wide range, depending on the formation and the state of the fibre and the test conditions. *Table 4* lists some typical values, after Morton and Hearle[13].

Figure 13 compares a stress–strain curve obtained in our laboratory for a nylon 66 sample with one derived using approach III.

The predictions based on approach I show a major effect of the mathematical form of averaging. Thus when the *moduli* are weighted according to parallel/series influence in *Figure 7*, the predicted moduli show a surprising independence of the amorphous modulus. The first set (from the left) with $P=0$ are not relevant since they are a pure series model. Of the rest, the only large

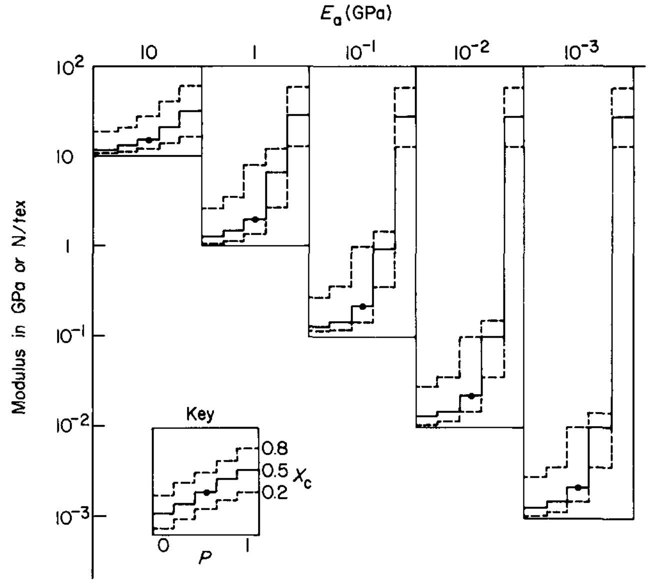

Figure 8 Computed initial modulus values under Approach I (based on weighted average of compliance)

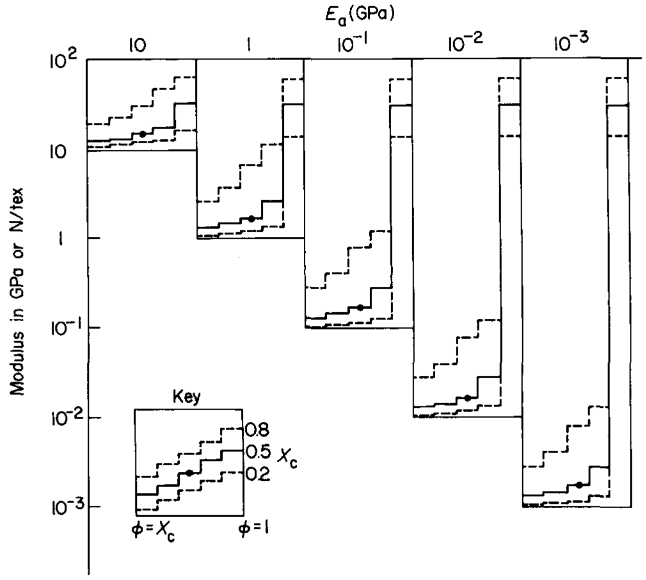

Figure 9 Computed initial modulus, series–parallel composite, values under Approach II presented as function of amorphous modulus, E_a, and for a fixed crystal modulus, E_c (100 GPa or N/Tex). Each set of values shows effect of crystallinity, X_c, and degree of parallel coupling, ϕ, on the composite modulus, e.g. solid line with a dot (–●–) represents modulus value for $\phi=0.75$ and $X_c=0.5$

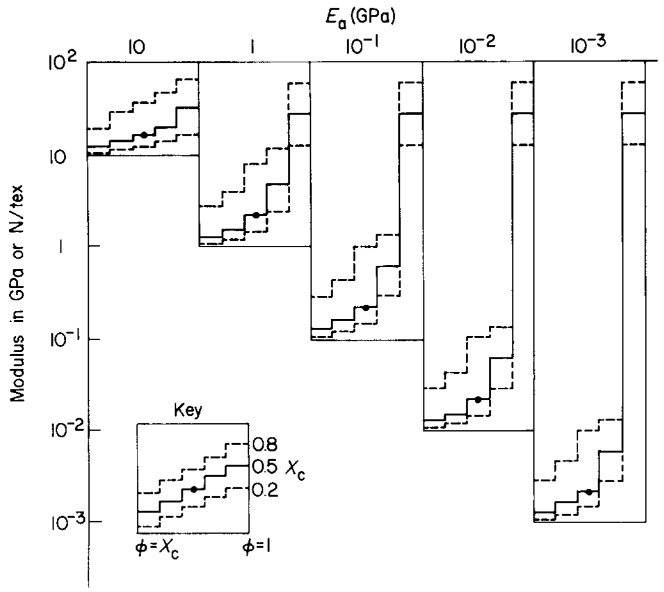

Figure 10 Computed initial modulus, parallel–series composite, values under Approach II

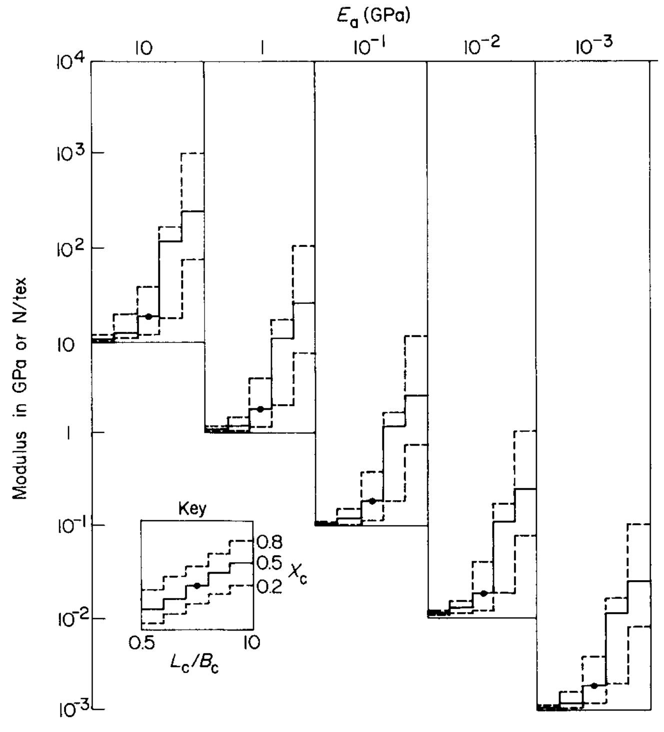

Figure 11 Computed initial modulus under Approach III, presented as a function of amorphous modulus, E_a. Each set shows effect of crystallinity, X_c, and crystal length to breadth ratio, L_c/B_c, e.g. solid line with a dot (–●–) represents modulus value for $L_c/B_c = 2$ and $X_c = 0.5$

differences occur at ($P = 0.2$, $X_c = 0.2$) between $E_a = 10$ and the lower values of E_a. There are small differences between $E_a = 10$ and the lower values of E_a over the range of values of P and X_c, and between $E_a = 1$ and lower values of E_a at the low combination $P = 0.2$, $X_c = 0.2$. The remainder are virtually identical over the different values of E_a.

Conversely, when the weighted *compliance* is used, *Figure 8*, it is the crystal modulus which has little influence, except at the extremes.

This sensitivity to the form of the mathematics complicates comparisons with experimental results, since fits tend to be forced to extreme values (in opposite directions, depending on the form of weighting). If there is modulus weighting, predicted moduli are all close to $0.1E_c$ except for very low values of P. If there is compliance weighting the predicted moduli are less than $10E_a$ except at very high values of P.

Approach II: modulus

Approach II is remarkable for the small influence of the sequence of calculation: in the middle of the range, the parallel–series modulus is only about 35% higher than

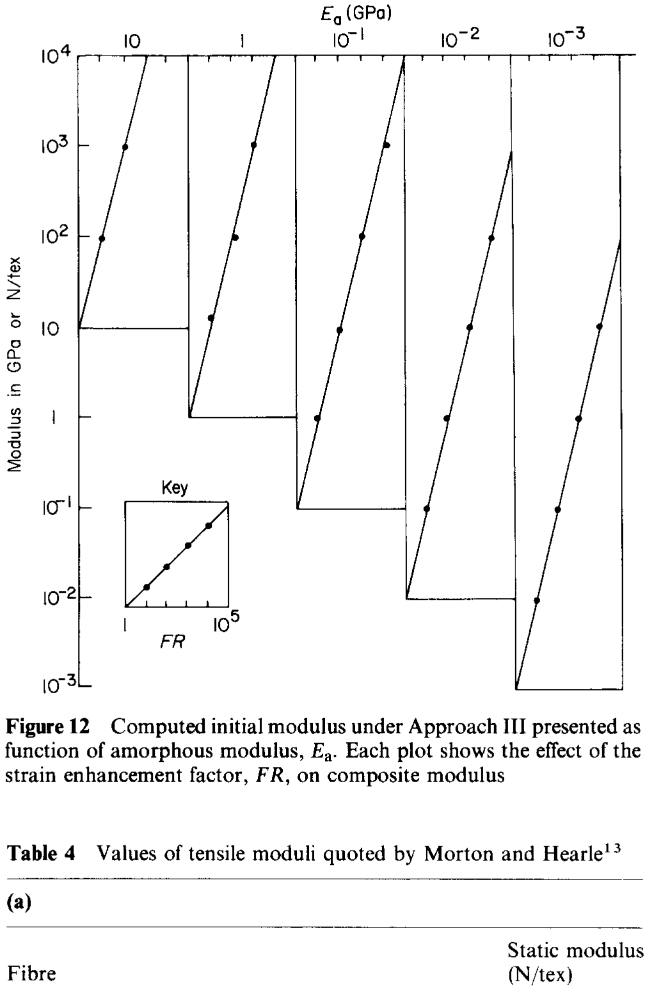

Figure 12 Computed initial modulus under Approach III presented as function of amorphous modulus, E_a. Each plot shows the effect of the strain enhancement factor, FR, on composite modulus

Table 4 Values of tensile moduli quoted by Morton and Hearle[13]

(a)

Fibre		Static modulus (N/tex)
Nylon-6,6		
	medium tenacity	3.0
	high tenacity	4.4
	staple fibre	1.0
Nylon-6	Perlon	0.6
Polyester fibre (Terylene)		
	medium tenacity	10.6
	high tenacity	13.2
	staple fibre	8.8

(b)

	Dynamic modulus (N/Tex)			
Fibre	20°C	100°C	150°C	Ref.
Nylon-6 (wet)	1.1	1.0	–	(17)
(dry)	3.5	2.3	1.2	(17)
Polyester				
(amorphous)	2.5	–	–	(18)
(dry)	15.1	9.5	3.3	(17)
(wet)	13.6	7.0	–	(17)

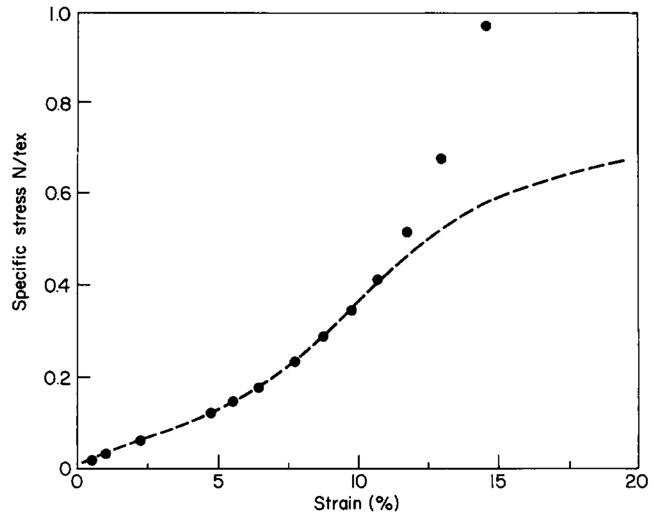

Figure 13 Experimental and theoretical stress–strain curves for a nylon-6,6 sample (Du Pont de Nemours Inc.)

the series–parallel value. The predictions are also very close to those for Approach I with compliance weighting, and are thus predominantly influenced by the value of E_a.

The predictions given by the alternative version of approach II, namely amorphous cuboidal inclusions in a crystal, have not been included, but are very similar to the predictions in *Figure 7* from approach I with modulus weighting, and are predominantly influenced by E_c. This would seem to suggest that the two predictions represent upper and lower bounds.

The predictions on approach II can certainly give values of the same order as the experimental results. With $X_c = 0.5$, and the middle value of ϕ, this would suggest an amorphous modulus in nylon of about 1 GPa. This is about ten times higher than the value estimated earlier in this paper. The discrepancy could be attributed *either* to amorphous orientation *or*, more probably, to the stiffening effect of crystalline material in the neighbouring unit.

The higher values for polyester would be attributed to the stiffening influence of the benzene rings.

Approach III

As the mathematical formulation suggests, the predicted moduli under this approach show a distinct dependence on E_a and on FR which is in turn derived from L_c/B_c and X_c. Here again the lower bound on modulus is given by $X_c = 0$ (or $L_c/B_c = 0$). But since this approach is independent of E_c or in other words assumes an infinite crystalline modulus, the upper bound should depend solely on L_c/B_c. The values predicted in the intermediate range ($L_c/B_c = 2$ and $X_c = 0.5$) are of the same order as given by Approach I with compliance weighting and Approach II. Since there cannot be a unique set of L_c/B_c and X_c values for a particular value of FR, we expect for example to have the same modulus for a system having 20% crystallinity with a length to breadth ratio of 5, and 50% crystallinity with a ratio of 2.

Using typical literature values of initial modulus for nylon yields FR in the range 5 to 50. This corresponds to crystal length to breadth ratios lying between 2:1 and 10:1. As shown in *Figure 13*, approach III describes very well the shape of a nylon stress–strain curve up to quite high strains (*ca.* 11%). A similar fit would also be given by approach I and II. Beyond this level it would be necessary to postulate some form of yielding mechanism associated, presumably, with the crystals. The fitting parameters used for this curve were $FR = 9.5$ and an initial modulus of 2.98 GPa compared with the measured value of 3.11 GPa. This would suggest a crystal length to breadth ratio of 4:1 for 50% crystallinity, which is in the expected range. It will be important to test the validity of this approach independently by a direct crystal size measurement.

CONCLUSIONS

The present exercise started with the intention of being a quick check of the Takayanagi approach to confirm that results of the right order of magnitude could be obtained. In fact it has shown up some complexities in handling a composite system.

The results confirm that a combination of crystalline material and an amorphous rubber expected from the chemical structure of nylon or polyester would give the observed stress–strain curves. No attempt has been made at precision in the parameters used, since the intention has been to indicate trends. For comparisons with properties of known samples, more precision would be attempted.

The similarities of the predictions of approaches I (with compliance weighting), II and III, with their strong dependence on amorphous modulus, suggest that they provide a basis for prediction. This implies a qualitative acceptance of a view that a material containing separate crystals embedded in a continuous amorphous matrix will deform under the major influence of the softer component, unless some special form of structure prevents this.

ACKNOWLEDGEMENTS

We would like to thank E. I. du Pont de Nemours, USA, for financial support for this work, and for supplying the yarn samples. We also wish to thank Mr D. Mwaisengela for performing the tensile tests.

REFERENCES

1 Hearle, J. W. S. and Greer, R. *Textile Progress* 1970, **2** (4), 53

2 Peterlin, A. *J. Mater. Sci.* 1971, **6**, 490

3 Prevorsek, D. C., Harget, P. J., Sharma, R. K. and Reimschuessel, A. C. *J. Macromol. Sci.* 1973, **B-8**, 127

4 Statton, W. O., private communication

5 Takayanagi, M. *Mem. Fac. Eng. Kyushu Univ.* 1963, **23**, 50

6 Treloar, L. R. G. *Polymer* 1960, **1**, 290

7 Treloar, L. R. G. 'Physics of Rubber Elasticity', 3rd Edn., Clarendon, Oxford, 1975, p. 120

8 Hearle, J. W. S. 'Polymers and Their Properties', Vol. 1, Ellis Horwood, Chichester, 1982, p. 223

9 Kuhn, W. and Grün, F. *Kolloid-Z.* 1942, **101**, 248; Kuhn, W. and Kuhn, H. *Helv. Chim. Acta* 1943, **26**, 1394; Kuhn, W. *Helv. Chim. Acta* 1946, **29**, 1095

10 James, H. M. and Guth, E. *J. Chem. Phys.* 1943, **11**, 470

11 Guth, E. *J. Appl. Phys.* 1945, **16**, 20

12 Mullins, L. and Tobin, N. R. *J. Appl. Polym. Sci.* 1965, **9**, 2993

13 Morton, W. and Hearle, J. W. S. 'Physical Properties of Textile Fibres', 2nd Edn., Heinemann, London, 1975, p. 283

14 Lyons, W. J. *J. Appl. Phys.* 1958, **29**, 1729

15 Wobser, G. and Blasenberg, S. *Kolloid Z.* 1970, **271**, 905

16 Dulmage, W. J. and Contois, L. E. *J. Polym. Sci.* 1958, **28**, 275

17 Van der Meer, S. J. 'Dynamic Mechanical Properties of Yarns – Cords and Plain Weave Fabrics', *Ph.D. Thesis*, De Technische Hogeschool, Delft, 1970

18 Thompson, J. H. and Wood, D. W. *Trans. Faraday Soc.* 1956, **52**, 1383